

# 000 001 002 003 004 005 006 007 008 009 010 011 012 013 014 015 016 017 018 019 020 021 022 023 024 025 026 027 028 029 030 031 032 033 034 035 036 037 038 039 040 041 042 043 044 045 046 047 048 049 050 051 052 053 SEViCES: UNIFYING SEMANTIC-VISUAL EVIDENCE CONSENSUS FOR LONG VIDEO UNDERSTANDING

Anonymous authors

Paper under double-blind review

## ABSTRACT

Long video understanding remains challenging due to its complex, diverse, and temporally scattered content. Although video large language models (Video-LLMs) can process videos lasting tens of minutes, applying them to truly long sequences is computationally prohibitive and often leads to unfocused or inconsistent reasoning. A promising solution is to select only the most informative frames, yet existing approaches typically ignore temporal dependencies or rely on unimodal evidence, limiting their ability to provide complete and query-relevant context. We propose a **Semantic–Visual Consensus Evidence Selection** (SeViCES) framework for effective and reliable long video understanding. SeViCES is training-free and model-agnostic, and introduces two key components. The Semantic–Visual Consensus Frame Selection (SVCFS) module selects frames through (1) a temporal-aware semantic branch that leverages LLM reasoning over captions, and (2) a cluster-guided visual branch that aligns embeddings with semantic scores via mutual information. The Answer Consensus Refinement (ACR) module further resolves inconsistencies between semantic- and visual-based predictions by fusing evidence and constraining the answer space. Extensive experiments on long video understanding benchmarks show that SeViCES consistently outperforms state-of-the-art methods in both accuracy and robustness, demonstrating the importance of consensus-driven evidence selection for Video-LLMs.

## 1 INTRODUCTION

Understanding long videos remains inherently challenging due to their complex, diverse, and temporally scattered content (Zou et al., 2024). Unlike short clips, long videos often span multiple events, scenes, and semantic contexts, making it difficult to capture a coherent global narrative (Wang et al., 2025a). Although recent video large language models (Video-LLMs) such as LLaVA-Video (Zhang et al., 2025d) and Qwen2.5-VL (Bai et al., 2025) demonstrate the ability to process videos lasting tens of minutes, their performance on truly long video understanding remains unsatisfactory. Directly feeding massive numbers of visual frames into Video-LLMs not only incurs prohibitive computational costs but also dilutes attention, often leading to unfocused reasoning and logically inconsistent interpretations (Zhang et al., 2025f).

A natural way to mitigate these limitations is to reduce the visual content input to Video-LLMs, allowing them to focus on the information most relevant to a query without relying on larger architectures or extensive fine-tuning. This raises a central challenge: *how to select the input visual content effectively*. The selected content must be both query-relevant and evidence-complete, filtering out redundant information while preserving the full reasoning chain required to answer the query. Existing solutions fall into two main categories: *token selection* and *frame selection*. Token selection methods (Zhang et al., 2025c;e; Shen et al., 2025a) reduce the number of visual tokens by estimating their importance or training a selector, but they typically require expensive fine-tuning or rely on layer-specific importance scores, which are not always consistent across layers. In contrast, frame selection methods (Liu et al., 2025a; Santos et al., 2025) choose a subset of frames before input to Video-LLMs. While efficient, naive strategies such as uniform sampling ignore query information, and similarity-based retrieval with VLMs like CLIP (Radford et al., 2021) improves query alignment but evaluates frames independently (Tang et al., 2025; Liu et al., 2025a), thereby overlooking temporal dependencies and contextual reasoning that are essential for evidence completeness.

In this light, we advance frame selection techniques for long video understanding, by developing a **Semantic-Visual Consensus Evidence Selection (SeViCES)** framework. SeViCES is training-free and model-agnostic, making it broadly applicable across different Video-LLMs. Our core insight is that long video understanding requires both identifying query-relevant and evidence-complete frames from complementary semantic and visual perspectives, and reconciling these perspectives into a consistent consensus. SeViCES enforces consensus at two levels: (1) **frame level**, where semantic and visual cues jointly guide selection, and (2) **answer level**, where discrepancies between Video-LLM’s outputs trigger adaptive refinement of both the selected frames and candidate answers.

To achieve this, SeViCES introduces two key innovations. First, the Semantic–Visual Consensus Frame Selection (SVCFS) module performs dual-perspective selection: (a) a Temporal-Aware Semantic Frame Selection (TAS-FS) branch that uses LLM scoring of captions with temporal context to capture semantic reasoning cues, and (b) a Cluster-guided Mutual Information Frame Selection (CgMI-FS) branch that aligns visual embeddings with semantic scores to ensure representativeness and diversity. Second, the Answer Consensus Refinement (ACR) module compares the answers produced from the two frame sets and resolves inconsistencies through evidence fusion and constrained decoding. Together, these components enable SeViCES to ensure that the final evidence set is both semantically and visually coherent, enabling accurate and consistent reasoning over long videos.

We summarize our contributions as follows:

- We propose SeViCES, a training-free, model-agnostic framework that unifies semantic and visual evidence for long video reasoning and enforces consensus at both frame and answer levels. Across four benchmarks, SeViCES consistently improves multiple Video-LLMs, achieving average gains of around 4.0% and up to 8.3% at best.
- We introduce two novel strategies for query-relevant and evidence-complete frame selection: Temporal-Aware Semantic Frame Selection based on LLM scoring of captions with temporal context, and Cluster-guided Mutual Information Frame Selection based on embedding-score alignment.
- We design an Answer Consensus Refinement module that explicitly uses inconsistencies between semantic- and visual-based predictions as signals to refine evidence and enforce robust consensus.

## 2 RELATED WORKS

**Token selection.** Token selection typically relies on indicators such as attention scores, semantic similarity, and contextual relevance to identify key tokens, thereby reducing the computational cost of large models. FrameFusion (Fu et al., 2024) first merges tokens with cosine similarity above a specified threshold at shallow layers, then calculates cumulative attention scores and applies top- $k$  importance pruning, effectively reducing the number of tokens. PruneVid (Huang et al., 2025) proposes to prune visual tokens through LLM attention computation, achieving substantial reductions in computational cost while preserving task performance. KVTP (Liu et al., 2025c) proposes a query-frame relevance predictor, which is trained to learn the contribution of frame pairs to the task, thereby dynamically determining the token pruning rate for each frame.

**Frame selection.** Early video-language models typically relied on uniform or fixed-interval frame sampling to construct visual inputs. Video-ChatGPT (Maaz et al., 2024), LLaMA-VID (Li et al., 2024) and LongVLM (Weng et al., 2024) adopt evenly spaced frames as visual evidence. While simple and efficient, such strategies often miss fine-grained or short-lived events, motivating the development of adaptive or query-guided frame selection methods.

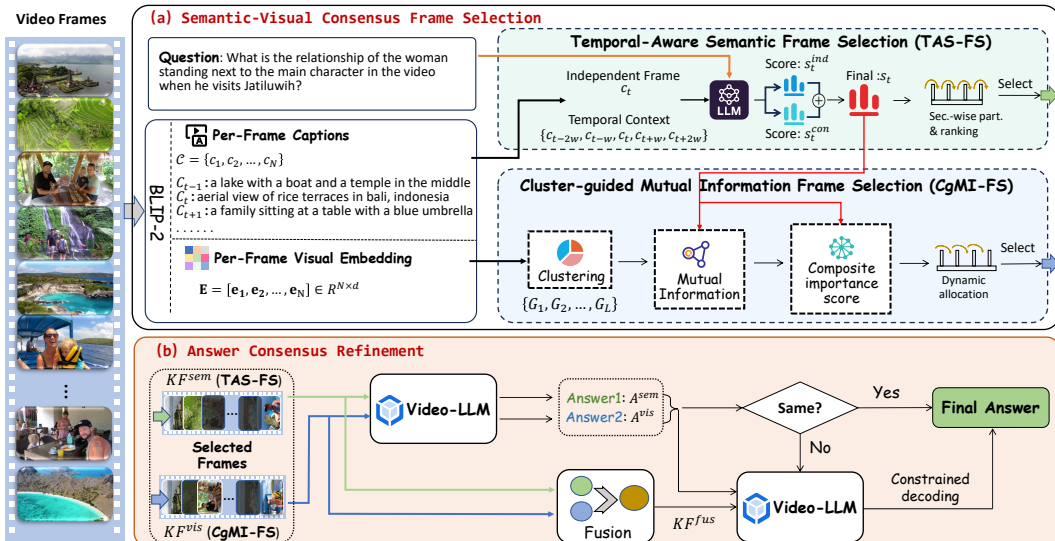
BOLT (Liu et al., 2025a) proposes leveraging inverse transform sampling to select query-relevant frames to improve VQA performance without requiring model retraining. MDP<sup>3</sup> (Sun et al., 2025) combines query-conditioned determinantal point processes with a Markov decision process to efficiently achieve diverse, query-relevant, and sequential frame selection. Frame-Voyager (Yu et al., 2025) extends frame selection by training on frame combinations rather than isolated frames, using prediction losses from a pretrained Video-LLM to rank candidate subsets, thereby capturing inter-frame interactions and temporal complementarities. DynFocus (Han et al., 2025) introduces a mechanism for dynamic event prototype estimation and compact cooperative encoding. It first distinguishes important frames from non-important ones, then applies fine-grained or coarse-grained

108 encoding accordingly. Two-stage training enables the modules to identify representative frames and  
 109 compress redundant ones while preserving critical details and temporal structure.  
 110

111 **Comparison with our work.** Unlike prior methods that focus solely on token compression or frame  
 112 subset selection, our approach is the first to introduce an evidence consensus perspective. Specifically,  
 113 SeViCES integrates both semantic and visual signals to achieve query-relevant and evidence-  
 114 complete frame selection, and further enforces answer-level consensus refinement by reconciling  
 115 discrepancies between semantic- and visual-based reasoning. This dual-level design enables Se-  
 116 ViCES to move beyond independent token or frame pruning, establishing a principled consensus-  
 117 driven framework for reliable long video reasoning.  
 118

### 3 METHODOLOGY

121 The overall framework of our SeViCES is illustrated in Figure 1. It consists of two key components:  
 122 Semantic-Visual Consensus Frame Selection (SVCFS) and Answer Consensus Refinement (ACR).  
 123 In the first stage, SVCFS adopts a dual-branch design that integrates complementary semantic and  
 124 visual cues to identify frames that are both query-relevant and evidence-complete, thereby con-  
 125 structing a reliable evidence pool for reasoning. In the second stage, ACR leverages the responses  
 126 of an MLLM conditioned on the two frame sets. By explicitly analyzing discrepancies between the  
 127 semantic-based and visual-based answers, ACR adaptively refines the selected frames and constrains  
 128 the prediction space to reconcile conflicts. This two-stage design distinguishes SeViCES from prior  
 129 frame selection methods: instead of relying on unimodal evidence or independent scoring, it estab-  
 130 lishes a consensus mechanism at both the frame and answer levels. The following sections detail  
 131 each component in turn.  
 132



149 Figure 1: The overall framework of our **SeViCES**. Video frames are processed by BLIP-2 to obtain  
 150 captions and embeddings. TAS-FS selects query-relevant frames from captions, while CgMI-FS  
 151 selects frames from embeddings. The two sets are then refined by the ACR module through evidence  
 152 fusion and constrained decoding to produce the final answer.  
 153

#### 3.1 SEMANTIC-VISUAL CONSENSUS FRAME SELECTION

155 Given a video  $V = f_1, \dots, f_{t-1}, f_t, f_{t+1}, \dots, f_N$  with  $N$  frames, the goal of SVCFS is to identify  
 156 a compact subset of frames (significantly fewer than  $N$ ) that jointly leverage semantic and visual  
 157 cues while preserving a complete and focused chain of evidence for answering a given question.  
 158 To this end, we design SVCFS as a dual-branch module: the semantic branch selects frames from  
 159 the perspective of semantic evidence, while the visual branch selects frames from the perspective of  
 160 visual evidence. Concretely, these correspond to two complementary strategies: **Temporal-Aware**  
 161 **Semantic Frame Selection** (TAS-FS) and **Cluster-guided Mutual Information Frame Selection**  
 (CgMI-FS), respectively.

162  
163

## 3.1.1 TEMPORAL-AWARE SEMANTIC FRAME SELECTION

164  
165  
166  
167  
168  
169  
170  
171  
172  
173

As discussed in prior works (Tang et al., 2025; Liu et al., 2025a), methods that rely on vision-language models (VLMs) such as CLIP to compute similarity scores between the question and frame features often struggle to identify strongly query-relevant frames. This limitation arises because CLIP-based similarity primarily captures surface-level alignment between visual content and declarative sentences, while effective frame selection for video question answering requires not only semantic matching but also contextual reasoning. For example, given the question “*What does the yellow turtle monster do after receiving a red book?*”, the relevant evidence may not only include the frame where the monster is holding the book, but also subsequent frames showing its follow-up actions. Such frames may not be semantically identical to the query description but are nevertheless essential for constructing the complete reasoning chain.

174  
175  
176  
177

To overcome this limitation, we replace CLIP-based similarity with an LLM-based relevance scoring strategy, leveraging the reasoning and information-matching capabilities of LLMs (e.g., Qwen2-7B-Instruct (Team, 2024)). Specifically, we first use a VLM (e.g., BLIP-2 (Li et al., 2023)) to generate a natural language caption  $c_t$  for each frame  $f_t$  as follows

178

$$\{c_1, c_2, \dots, c_N\}, [e_1, e_2, \dots, e_N] = \text{BLIP-2}(f_1, f_2, \dots, f_N), \quad (1)$$

179  
180  
181  
182

where the embeddings  $\mathbf{E}$  are later consumed by the visual branch. These captions are then evaluated by an LLM to produce a semantic relevance score with respect to the question  $Q$ . To capture both local detail and contextual reasoning, we design two complementary scoring strategies:

183

$$s_i^{ind} = \text{LLM}(Q, c_t; \text{prompt}_{ind}), \quad (2)$$

184  
185

$$s_i^{con} = \text{LLM}(Q, \{c_{t-2w}, c_{t-w}, c_t, c_{t+w}, c_{t+2w}\}; \text{prompt}_{con}), \quad (3)$$

186  
187  
188  
189  
190  
191

where  $\text{prompt}_{ind}$  and  $\text{prompt}_{con}$  are the instruction prompts for the two modes, respectively. The scores are required to be in the range  $[0, 10]$ . The frame-independent scoring evaluates each frame solely from its own caption, while the temporal-context scoring incorporates neighboring captions within a stride- $w$  window, enabling the LLM to reason about causal dependencies, abstract concepts, and temporal transitions. Finally, the semantic relevance score of each frame is obtained by combining the two scoring strategies:

192

$$s_t = s_t^{ind} + s_t^{con}, \quad (4)$$

193  
194  
195

which balances fine-grained local alignment with broader temporal reasoning, ensuring both query relevance and evidence completeness.

196  
197  
198  
199  
200  
201  
202  
203  
204

After computing the semantic scores for all frames, a straightforward approach is to directly select the top- $M$  frames with the highest scores. However, such ranking may overconcentrate selections in certain segments, missing critical evidence elsewhere. To mitigate this, we propose a hybrid selection strategy combining global ranking with section-wise partitioning. Specifically, the video is first divided into four equal temporal sections. Within each section, we select the top- $P$  frames ( $P < \frac{M}{4}$ ) by score to guarantee local evidence coverage. From the remaining frames across the entire video, we then select the top- $(M - 4P)$  frames globally. This two-step procedure ensures both temporal diversity and global relevance, thereby improving the completeness of the selected evidence.

205  
206

## 3.1.2 CLUSTER-GUIDED MUTUAL INFORMATION FRAME SELECTION

207  
208  
209  
210

Visual embeddings provide another crucial modality for video representation, since frame captions alone cannot fully capture the richness of visual content. To complement the semantic branch, we introduce a Cluster-guided Mutual Information Frame Selection (CgMI-FS), which leverages frame embeddings  $\mathbf{E} \in \mathbb{R}^{N \times d}$  to incorporate visual evidence.

211  
212  
213  
214  
215

Specifically, we first cluster the BLIP-2-generated embeddings of all  $N$  frames to obtain groups of visually related frames. For clustering, we adopt an improved Density Peaks Clustering (DPC) algorithm (Du et al., 2016) enhanced with K-Nearest Neighbor (KNN) distance computation, which partitions the frame embeddings into compact groups in an unsupervised manner. Each cluster center represents a local mode of the global content distribution, and the distance between a frame embedding  $\mathbf{E}_i$  and its corresponding cluster center provides a measure of membership strength. As

216 a result, the  $N$  frames are partitioned into  $L$  clusters  $G_1, G_2, \dots, G_L$ , which capture the coarse-  
217 grained distribution of visual content across the video.

218 However, clustering alone does not account for the query and thus cannot directly capture relevance.  
219 To address this, we further integrate semantic-based relevance information (from LLM-scored captions)  
220 into the clustered structure via a mutual information strategy, which aligns clusters with the  
221 question and highlights visually representative frames that contribute to query-relevant evidence.  
222 Concretely, for cluster  $G_i$  with  $N^i$  frames, let its embeddings be  $\mathbf{E}^i$  and their semantic scores be  
223  $\mathbf{s}^i = [s_1^i, s_2^i, \dots, s_{N^i}^i]$ . We first reduce  $\mathbf{E}^i$  to  $\hat{\mathbf{E}}^i \in \mathbb{R}^{N^i \times d'}$  using PCA, preserving 95% of the  
224 variance. We then compute the mutual information (Kraskov et al., 2004) between each reduced  
225 embedding dimension and the semantic scores:

$$227 \quad MI_j^i = \text{Mutual-Information}(\hat{\mathbf{E}}_{\cdot|j}^i, \mathbf{s}^i), \quad MI^i = \sum_{j \in d'} MI_j^i. \quad (5)$$

229 Next, we define a composite importance score  $IM$  for each cluster  $i$ :

$$230 \quad IM^i = (1 + MI^i) \cdot \bar{s} \cdot \epsilon + \frac{\sigma^2}{2}, \text{ where } \epsilon = 1 - \frac{1}{N^i} \sum_{j \in N^i} \text{sim}(\mathbf{e}_i^{\text{center}}, \mathbf{e}_j^{\text{center}}) \quad (6)$$

233  $\bar{s}$  is the average semantic score within the cluster,  $\sigma^2$  is the score variance, and  $\epsilon$  measures the  
234 distinctiveness of cluster  $i$  with respect to others. This composite score integrates query relevance,  
235 intra-cluster diversity, and inter-cluster distinctiveness. Finally, we perform dynamic allocation of  
236 the target frame budget (e.g.,  $M = 64$ ) to clusters based on their importance scores:

$$237 \quad M^i = \text{Round} \left( M \times \frac{IM^i}{\sum_j IM^j} \right). \quad (7)$$

240 For each cluster  $i$ , the top- $M^i$  frames are then selected according to their semantic scores  $s$ .

241 This multi-level selection strategy ensures that the final keyframe set balances query relevance,  
242 visual representativeness, and contextual diversity, thereby providing a high-quality evidence pool  
243 for long video question answering.

### 245 3.2 ANSWER CONSENSUS REFINEMENT

247 SVCFS produces two sets of keyframes,  $KF^{sem}$  and  $KF^{vis}$ , which reflect complementary semantic  
248 and visual perspectives of the video. Although both are designed to capture question-relevant  
249 evidence, they may emphasize different aspects of the content. Instead of directly fusing these sets  
250 at the frame level, we propose an Answer Consensus Refinement (ACR) strategy that evaluates the  
251 answers produced by Video-LLMs when conditioned on each set, and uses their agreement or dis-  
252 agreement as a signal for refinement. The central idea is to treat answer inconsistency as evidence  
253 incompleteness, and to resolve it through targeted reasoning.

254 Formally, given a question  $Q$ , we obtain two initial answers by inputting each keyframe set into the  
255 MLLM:

$$256 \quad A^{sem} = \text{Video-LLM}(Q; KF^{sem}), \quad A^{vis} = \text{Video-LLM}(Q; KF^{vis}). \quad (8)$$

257 For multiple-choice questions (as in many benchmarks), we assess their consistency by checking  
258 whether the predicted option indices coincide. If  $A^{sem} = A^{vis}$ , we regard the agreement as a sign  
259 of high confidence and accept the answer directly.

260 When the two answers diverge, ACR initiates a refinement process consisting of two steps: evidence  
261 fusion and candidate-restricted inference.

262 **Evidence fusion.** We construct a fused set of keyframes  $KF^{fus}$  by taking the union of  $KF^{sem}$  and  
263  $KF^{vis}$ :

$$264 \quad KF^{fus} = KF^{sem} \cup KF^{vis}. \quad (9)$$

265 This fusion aggregates all unique evidence identified by the two selection strategies, ensuring that  
266 the MLLM has access to a richer and more complete context.

267 **Constrained decoding.** Rather than re-predicting over the entire answer space, we constrain the  
268 MLLM to adjudicate between the two conflicting candidates  $A^{sem}$  and  $A^{vis}$ . That is,

$$269 \quad A = \text{Video-LLM}(Q; KF^{sem} \cup KF^{vis}; \text{Answer candidates:}\{A^{sem}, A^{vis}\}). \quad (10)$$

270 This restriction forces the model into a comparative reasoning process, explicitly evaluating which  
 271 answer is better supported by the fused evidence.

272 By converting disagreement into a constructive signal, ACR enforces answer-level consensus, re-  
 273 duces ambiguity, and ensures more accurate and robust predictions for long video understanding.

## 274 4 EXPERIMENTS

### 275 4.1 EXPERIMENTAL SETUP AND DETAILS

276 **Dataset and evaluation.** We conduct our experiment on four long video understanding datasets.  
 277 MLVU (Zhou et al., 2025) contains nine video categories, including movies, surveillance, and oth-  
 278 ers, with durations ranging from three minutes to two hours. The MLVU dev set includes over  
 279 1,100 videos and 2,174 corresponding questions. MLVU’s overall score is computed as the average  
 280 accuracy across all task categories. VideoMME (Fu et al., 2025) consists of short-, medium-, and  
 281 long-duration videos. Each category contains 300 videos, with three questions per video, result-  
 282 ing in a total of 2,700 questions covering six major domains such as knowledge, film, and sports.  
 283 LongVideoBench (Wu et al., 2024) provides a validation set with more than 700 videos and 1,337  
 284 questions. The questions are categorized into two levels—perception and relation—and further di-  
 285 vided into 17 fine-grained subcategories. LVbench (Wang et al., 2025b) consists of 103 videos with  
 286 an average duration exceeding one hour, accompanied by 1,549 multiple-choice questions. It is  
 287 specifically designed to evaluate models’ capability to process ultra-long videos.

288 **Implementation details.** We integrate the proposed method as a plug-and-play module into several  
 289 open-source MLLMs, namely LLaVA-Video (Zhang et al., 2025d), Qwen2.5-VL (Bai et al., 2025),  
 290 and InternVL2.5 (Chen et al., 2025), to evaluate its effectiveness. As the baseline, these models  
 291 uniformly sample 64 frames from each video for inference. In contrast, our method determines the  
 292 sampling strategy according to video length defined by the benchmarks: for videos shorter than two  
 293 minutes, we uniformly sample 128 frames; for videos between two and fifteen minutes, we sample  
 294 at 1 fps; and for longer videos, we directly sample 1,024 frames uniformly. From these initially  
 295 sampled frames, we then apply our filtering approach to obtain two distinct sets of 64 frame indices  
 296 for each query.

300 Table 1: Performance comparison between our SeViCES and existing methods on four datasets.

301 Model	302 Size	303 Frames	304 VideoMME			305 MLVU	306 LongVB	307 LVBench
			308 Medium	309 Long	310 Overall			
<i>Proprietary Models</i>								
GPT-4o	—	384	70.3	65.3	71.9	64.6	<b>66.7</b>	<b>48.9</b>
Gemini-1.5-Pro	—	1 fps	<b>74.3</b>	<b>67.4</b>	<b>75.0</b>	—	64.0	33.1
<i>Open-Source VideoLLMs</i>								
mPLUG-Owl3	7B	128	57.7	50.1	59.3	63.7	52.1	43.5
NVILA	8B	256	62.2	54.8	64.2	70.1	57.7	—
VideoLLaMA3	7B	180	63.7	54.9	66.2	73.0	59.8	45.3
Oryx-1.5	32B	128	<u>65.3</u>	<u>59.3</u>	<u>67.3</u>	72.3	62.0	30.8
Video-XL-Pro	3B	240	—	—	60.0	70.6	56.7	—
SF-LLaVA-1.5	7B	128	—	—	63.9	71.5	62.5	45.3
LongVU	7B	1 fps	—	<b>59.5</b>	60.6	65.4	—	—
ViLAMP	7B	1 fps	<b>65.8</b>	57.8	<b>67.5</b>	72.6	61.2	45.2
Qwen2.5-VL	7B	64	62.6	53.1	63.5	63.9	60.2	41.0
+ SeViCES (Ours)	7B	64	<u>65.3</u> <u>↑2.7</u>	<u>56.8</u> <u>↑3.7</u>	<u>65.5</u> <u>↑2.0</u>	<u>72.2</u> <u>↑8.3</u>	<u>63.9</u> <u>↑3.7</u>	<u>45.4</u> <u>↑4.4</u>
LLaVA-Video	7B	64	62.3	53.0	64.4	67.9	58.9	43.1
+ AKS	7B	64	—	—	65.3	—	62.7	—
+ Suo et al. (2025)	7B	32	—	—	66.5	<b>73.4</b>	61.4	46.1
+ SeViCES (Ours)	7B	64	<u>64.7</u> <u>↑2.4</u>	<u>56.1</u> <u>↑3.1</u>	<u>65.6</u> <u>↑1.2</u>	<u>73.1</u> <u>↑5.2</u>	<u>63.1</u> <u>↑4.2</u>	<u>47.3</u> <u>↑4.2</u>
InternVL2.5	8B	64	—	52.8	64.2	68.7	59.3	43.4
+ Suo et al. (2025)	8B	32	—	—	65.3	70.0	60.6	46.6
+ SeViCES (Ours)	8B	64	63.2	<u>55.2</u> <u>↑2.4</u>	<u>64.7</u> <u>↑0.5</u>	<u>72.1</u> <u>↑3.4</u>	<u>61.7</u> <u>↑2.4</u>	<u>46.7</u> <u>↑3.3</u>

324 4.2 RESULTS AND ANALYSIS  
325

326 We evaluate our method by comparing the performance of recent mainstream proprietary and open-  
327 source multimodal large language models (MLLMs) across four long video understanding benchmarks.  
328 The proprietary models include *GPT-4o* (Hurst et al., 2024) and *Gemini-1.5-Pro* (Team et al.,  
329 2024). The open-source models include *mPLUG-Owl3* (Ye et al., 2025), *NVILA* (Liu et al., 2025d),  
330 *VideoLLaMA3* (Zhang et al., 2025a), *Oryx-1.5* (Liu et al., 2025e), *Video-XL-Pro* (Liu et al., 2025b),  
331 *SF-LLaVA-1.5* (Xu et al., 2025), *LongVU* (Shen et al., 2025b), and *ViLAMP* (Cheng et al., 2025).

332 4.2.1 COMPARISON WITH STATE-OF-THE-ARTS  
333

334 Table 1 reports the results across the four datasets. We have the following observations:  
335

336 **Effectiveness and generalization of SeViCES.** When integrated into three different Video-LLMs,  
337 SeViCES consistently delivers substantial performance gains across all benchmarks. For instance,  
338 on Video-MME, Qwen2.5-VL with SeViCES improves accuracy by 2.7% on medium-duration  
339 videos (~10 minutes) and by 3.7% on long-duration videos (~40 minutes) compared with uniform  
340 64-frame sampling. On MLVU, LongVB, and LVBench, SeViCES achieves additional gains  
341 of 8.3%, 3.7%, and 4.4%, respectively. These results demonstrate that SeViCES is both effective in  
342 selecting informative frames and broadly generalizable across different Video-LLMs.

343 **Comparison with other training-free frame selection methods.** AKS (Tang et al., 2025) and  
344 Suo et al. (2025) are representative training-free frame selection methods. Compared with AKS,  
345 SeViCES consistently performs better across all datasets with the baseline LLaVA-Video. Against  
346 Suo et al. (2025), SeViCES achieves superior results on most benchmarks: it is slightly weaker  
347 on Video-MME but obtains consistently higher performance on LongVB and LVBench across both  
348 LLaVA-Video and InternVL2.5 backbones. Considering that Suo et al. (2025) heavily relies on  
349 repeated LLM and Video-LLM calls, SeViCES achieves these improvements with higher efficiency.

350 **Comparison with open-source Video-LLMs.** By equipping Video-LLMs with SeViCES, their  
351 performance surpasses many open-source models, even when using only 64 frames. For example,  
352 Qwen2.5-VL (7B) combined with SeViCES significantly outperforms Oryx-1.5 (32B) on MLVU,  
353 LongVB, and LVBench, highlighting the efficiency and scalability advantages of our approach.

354 4.2.2 PERFORMANCE ACROSS VIDEO TASK TYPES  
355

356 Figure 2 compares the performance of LLaVA-Video and Qwen2.5-VL on the LVBench dataset,  
357 both with and without SeViCES, across five distinct video understanding tasks: information  
358 retrieval, event understanding, entity recognition, reasoning, and temporal grounding. Notably, on  
359 the Key Information Retrieval task, Qwen2.5-VL improves from 39.9% to 50.2% accuracy, showing  
360 that SeViCES effectively identifies and preserves frames containing information critical to the  
361 query. This highlights the ability of our selection strategy to filter noise while retaining content most  
362 relevant for precise retrieval. When averaging results across LLaVA-Video and Qwen2.5-VL, we  
363 observe gains of 5.5% on the Entity Recognition task and 3.2% on the Event Understanding task.  
364 These improvements indicate that SeViCES enhances the models’ ability to capture key scenes, fol-  
365 low event progression, and track entities, which in turn enables clearer reasoning and more accurate  
366 temporal analysis.

367 4.3 ABLATION STUDY  
368

369 In the ablation study, we examine the effects of SeViCES components and some hyper-parameters  
370 using Qwen2.5-VL baseline and VideoMME dataset.

371 **Effect of key components of SeViCES.** SeViCES consists of two main components: Semantic-  
372 Visual Consensus Frame Selection (SVCFS) and Answer Consensus Refinement (ACR). SVCFS  
373 integrates two complementary strategies, i.e., Temporal-Aware Semantic Frame Selection (TAS-FS)  
374 and Cluster-guided Mutual Information Frame Selection (CgMI-FS), to identify frames. To eval-  
375 uate their contributions, we feed the frame sets generated by TAS-FS and CgMI-FS separately into  
376 Qwen2.5-VL. As shown in Table 2, both TAS-FS and CgMI-FS yield substantial improvements over  
377 the baseline across all settings. In particular, on the long-video setting (average duration ~40 min-  
utes), TAS-FS improves accuracy by 1.7%, while CgMI-FS achieves a much higher 3.1% gain. This

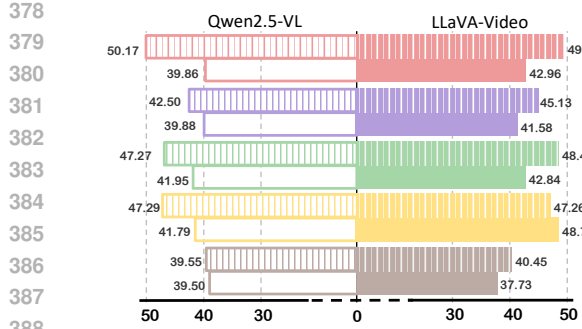


Figure 2: Performance of LLaVA-Video and Qwen2.5-VL on LVBench tasks with and without SeViCES. Task types include Key Information Retrieval (KIR), Event Understanding (EU), Entity Recognition (ER), Reasoning (Rea), and Temporal Grounding (TG).

Table 2: Performance changes of different SeViCES components.

Method	Overall	Medium	Long
Qwen2.5-VL	63.5	62.6	53.1
+ SVCFS (TAS-FS)	64.4 $\uparrow 0.9$	64.3 $\uparrow 1.7$	54.8 $\uparrow 1.7$
+ SVCFS (CgMI-FS)	64.4 $\uparrow 0.9$	63.9 $\uparrow 1.3$	56.2 $\uparrow 3.1$
+ SVCFS+ACR	65.5 $\uparrow 2.0$	65.3 $\uparrow 2.8$	56.8 $\uparrow 3.7$

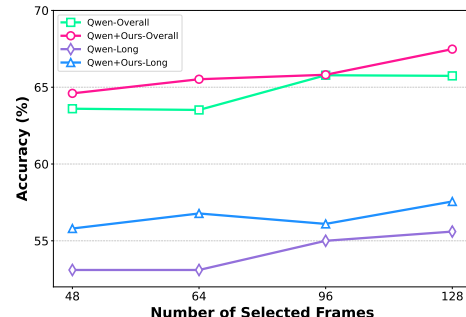


Figure 3: Performance changes with different numbers of selected frames.

Table 3: Performance changes with different number  $L$  of clusters.

Method	Overall	Medium	Long
Qwen2.5-VL	63.5	62.6	53.1
$L=8$	64.3	62.6	55.6
$L=12$	64.4	63.9	56.2
$L=16$	64.2	64.7	55.8

demonstrates that SVCFS effectively identifies key frames even under challenging long-duration scenarios. Furthermore, incorporating ACR for answer-level refinement brings additional improvements, confirming that consensus-based adjudication helps resolve ambiguities and enhances robustness.

**Effect of the number  $M$  of selected frames.** The number of input frames  $M$  has a direct impact on answer accuracy. We evaluate Qwen2.5-VL with  $M \in 48, 64, 96, 128$ . As shown in Figure 3, accuracy generally improves as more frames are provided. When SeViCES is applied, performance increases steadily across all settings, consistently surpassing the baseline. Notably, even in cases where baseline accuracy plateaus or slightly fluctuates with larger  $M$ , SeViCES maintains clear advantages. These results demonstrate that our semantic–visual consensus strategy scales effectively with frame budget and yields robust improvements over uniform sampling.

**Effect of the number  $L$  of clusters in CgMI-FS.** CgMI-FS groups frames via clustering, making the number of clusters  $L$  a critical hyper-parameter. We evaluate three settings ( $L = 8, 12, 16$ ) and report their results in Table 3. Two key observations emerge: (1) clustering consistently improves performance over the baseline, regardless of the chosen  $L$ , confirming the effectiveness of modeling global visual structure; and (2) among the tested values,  $L = 12$  achieves the best balance, yielding superior results on both the long-video and overall settings. Therefore, we adopt  $L = 12$  as the default configuration in the experiments.

#### 4.4 EXAMPLE DEMONSTRATION

To visually demonstrate the complementary strengths of the semantic- and visual-based frame selection strategies (TAS-FS and CgMI-FS), as well as the effectiveness of the answer refinement module (ACR), we present two representative video QA cases: (1) a single-correct multiple-choice question and (2) an elimination-type multiple-choice question.

For the single-correct question (Figure 4(1)), the query is: “*What does the yellow turtle monster do after receiving a red book?*”. The critical cues include both the “yellow turtle monster” and the “red book”, and the answer depends on selecting frames that occur “*after the book is received*”. In

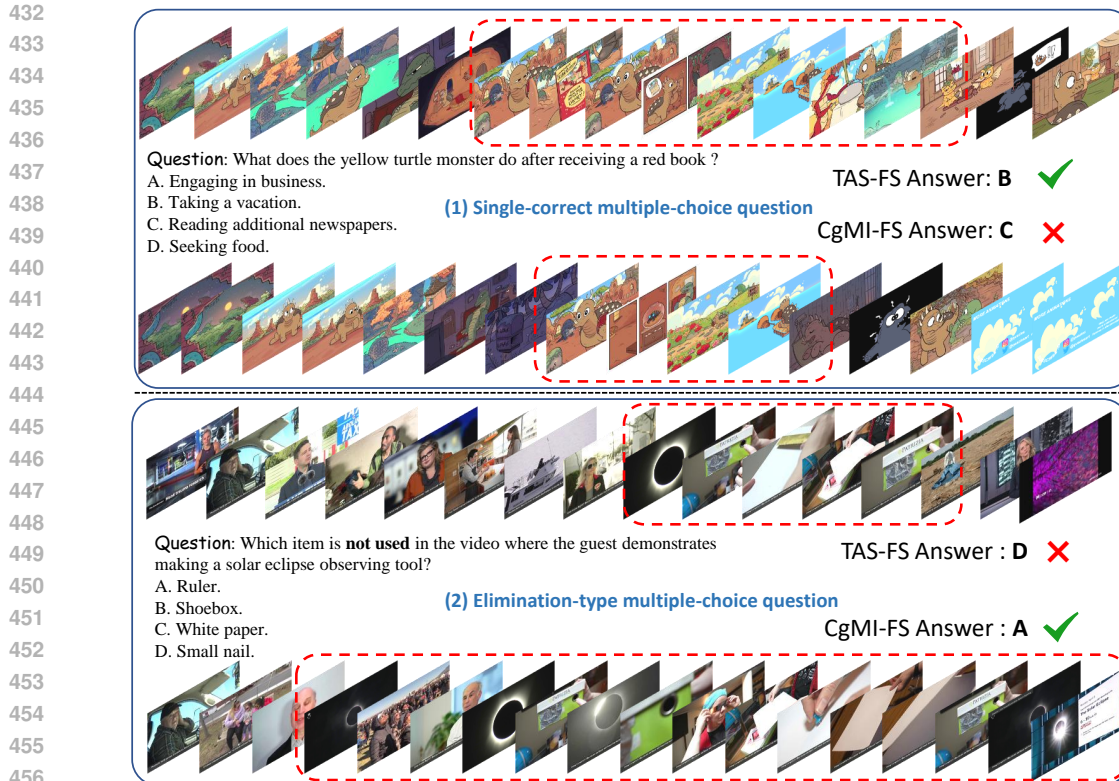


Figure 4: Two representative VideoQA task examples using Qwen2.5-VL and VideoMME dataset.

practice, the LLM-based TAS-FS successfully identifies frames capturing this temporal dependency, highlighting both the object and its subsequent action. In contrast, the clustering-based CgMI-FS primarily selects frames containing the yellow turtle monster but often overlooks the red book, likely because the book appears only briefly and co-occurs with the monster.

For the elimination-type question (Figure 4(2)), the query is: *“Which item is not used in the video where the guest demonstrates making a solar eclipse observing tool?”*. This task requires identifying all relevant objects in the video. Here, the clustering-based CgMI-FS, which models global visual distributions, excels at capturing a diverse set of objects, making it more effective than TAS-FS alone.

Finally, when the frame sets from TAS-FS and CgMI-FS are fused, the ACR module resolves their discrepancies and guides the Video-LLM to the correct final answer. These case studies illustrate how TAS-FS and CgMI-FS provide complementary evidence, i.e., semantic reasoning for temporal dependencies and visual clustering for global coverage, and how ACR integrates them into a robust consensus.

## 5 CONCLUSION

We have introduced SeViCES, a training-free and model-agnostic framework for long video understanding with Video-LLMs. By combining semantic-visual consensus frame selection (SVCFS) and answer consensus refinement (ACR), SeViCES ensures that selected frames are both query-relevant and evidence-complete, while inconsistencies between semantic and visual reasoning are turned into constructive signals for refinement. Experiments across multiple benchmarks show that SeViCES consistently boosts accuracy and robustness over strong baselines and existing training-free methods, even with limited frame budgets. Our analysis further demonstrates the scalability of the approach and its generalizability across different Video-LLMs. These results highlight the promise of consensus-driven evidence selection as a principled strategy for improving the reliability of long video understanding.

486 REFERENCES  
487

488 Shuai Bai, Keqin Chen, Xuejing Liu, Jialin Wang, Wenbin Ge, Sibo Song, Kai Dang, Peng Wang,  
489 Shijie Wang, Jun Tang, et al. Qwen2.5-v1 technical report. *arXiv preprint arXiv:2502.13923*,  
490 2025.

491 Zhe Chen, Weiyun Wang, Yue Cao, Yangzhou Liu, Zhangwei Gao, Erfei Cui, Jinguo Zhu, Shen-  
492 glong Ye, Hao Tian, Zhaoyang Liu, et al. Expanding performance boundaries of open-source  
493 multimodal models with model, data, and test-time scaling. *arXiv preprint arXiv:2412.05271*,  
494 2025.

495 Chuanqi Cheng, Jian Guan, Wei Wu, and Rui Yan. Scaling video-language models to 10k frames  
496 via hierarchical differential distillation. In *Forty-second International Conference on Machine  
497 Learning*, 2025. URL <https://openreview.net/forum?id=1CK1kuH1he>.

498 Mingjing Du, Shifei Ding, and Hongjie Jia. Study on density peaks clustering based on k-nearest  
499 neighbors and principal component analysis. *Knowledge-Based Systems*, 99:135–145, 2016.

500 Chaoyou Fu, Yuhua Dai, Yongdong Luo, Lei Li, Shuhuai Ren, Renrui Zhang, Zihan Wang, Chenyu  
501 Zhou, Yunhang Shen, Mengdan Zhang, et al. Video-mme: The first-ever comprehensive eval-  
502 uation benchmark of multi-modal llms in video analysis. In *Proceedings of the Computer Vision  
503 and Pattern Recognition Conference*, pp. 24108–24118, 2025.

504 Tianyu Fu, Tengxuan Liu, Qinghao Han, Guohao Dai, Shengen Yan, Huazhong Yang, Xuefei Ning,  
505 and Yu Wang. Framefusion: Combining similarity and importance for video token reduction on  
506 large visual language models. *arXiv preprint arXiv:2501.01986*, 2024.

507 Yudong Han, Qingpei Guo, Liyuan Pan, Liu Liu, Yu Guan, and Ming Yang. Dynfocus: Dynamic  
508 cooperative network empowers llms with video understanding. In *Proceedings of the Computer  
509 Vision and Pattern Recognition Conference*, pp. 8512–8522, 2025.

510 Xiaohu Huang, Hao Zhou, and Kai Han. PruneVid: Visual token pruning for efficient video large  
511 language models. In *Findings of the Association for Computational Linguistics: ACL 2025*, pp.  
512 19959–19973, Vienna, Austria, July 2025. Association for Computational Linguistics. ISBN 979-  
513 8-89176-256-5. doi: 10.18653/v1/2025.findings-acl.1024. URL <https://aclanthology.org/2025.findings-acl.1024/>.

514 Aaron Hurst, Adam Lerer, Adam P Goucher, Adam Perelman, Aditya Ramesh, Aidan Clark, AJ Os-  
515 trow, Akila Welihinda, Alan Hayes, Alec Radford, et al. Gpt-4o system card. *arXiv preprint  
516 arXiv:2410.21276*, 2024.

517 Alexander Kraskov, Harald Stögbauer, and Peter Grassberger. Estimating mutual information. *Phys-  
518 ical Review E—Statistical, Nonlinear, and Soft Matter Physics*, 69(6):066138, 2004.

519 Junnan Li, Dongxu Li, Silvio Savarese, and Steven Hoi. Blip-2: Bootstrapping language-image  
520 pre-training with frozen image encoders and large language models. In *International conference  
521 on machine learning*, pp. 19730–19742. PMLR, 2023.

522 Yanwei Li, Chengyao Wang, and Jiaya Jia. Llama-vid: An image is worth 2 tokens in large language  
523 models. In *European Conference on Computer Vision*, pp. 323–340. Springer, 2024.

524 Shuming Liu, Chen Zhao, Tianqi Xu, and Bernard Ghanem. Bolt: Boost large vision-language  
525 model without training for long-form video understanding. In *Proceedings of the Computer Vision  
526 and Pattern Recognition Conference*, pp. 3318–3327, 2025a.

527 Xiangrui Liu, Yan Shu, Zheng Liu, Ao Li, Yang Tian, and Bo Zhao. Video-xl-pro: Reconstructive  
528 token compression for extremely long video understanding. *arXiv preprint arXiv:2503.18478*,  
529 2025b.

530 Yudong Liu, Jingwei Sun, Yueqian Lin, Jingyang Zhang, Ming Yin, Qinsi Wang, Jianyi Zhang,  
531 Hai Li, and Yiran Chen. Keyframe-oriented vision token pruning: Enhancing efficiency of large  
532 vision language models on long-form video processing. *arXiv preprint arXiv:2503.10742*, 2025c.

540 Zhijian Liu, Ligeng Zhu, Baifeng Shi, Zhuoyang Zhang, Yuming Lou, Shang Yang, Haocheng Xi,  
 541 Shiyi Cao, Yuxian Gu, Dacheng Li, et al. Nvila: Efficient frontier visual language models. In  
 542 *Proceedings of the Computer Vision and Pattern Recognition Conference*, pp. 4122–4134, 2025d.  
 543

544 Zuyan Liu, Yuhao Dong, Ziwei Liu, Winston Hu, Jiwen Lu, and Yongming Rao. Oryx MLLM:  
 545 On-demand spatial-temporal understanding at arbitrary resolution. In *The Thirteenth Interna-*  
 546 *tional Conference on Learning Representations*, 2025e. URL [https://openreview.net/](https://openreview.net/forum?id=ODiY6pbHZQ)  
 547 [forum?id=ODiY6pbHZQ](https://openreview.net/forum?id=ODiY6pbHZQ).

548 Muhammad Maaz, Hanoona Rasheed, Salman Khan, and Fahad Khan. Video-chatgpt: Towards  
 549 detailed video understanding via large vision and language models. In *Proceedings of the 62nd*  
 550 *Annual Meeting of the Association for Computational Linguistics (Volume 1: Long Papers)*, pp.  
 551 12585–12602, 2024.

552 Alec Radford, Jong Wook Kim, Chris Hallacy, Aditya Ramesh, Gabriel Goh, Sandhini Agarwal,  
 553 Girish Sastry, Amanda Askell, Pamela Mishkin, Jack Clark, et al. Learning transferable visual  
 554 models from natural language supervision. In *International conference on machine learning*, pp.  
 555 8748–8763. PMLR, 2021.

556 Saul Santos, António Farinhas, Daniel C McNamee, and Andre Martins. \$\backslash\$infty\$-video: A training-  
 557 free approach to long video understanding via continuous-time memory consolidation. In *Forty-*  
 558 *second International Conference on Machine Learning*, 2025. URL [https://openreview.net/](https://openreview.net/forum?id=afDHwQ1ZDO)  
 559 [forum?id=afDHwQ1ZDO](https://openreview.net/forum?id=afDHwQ1ZDO).

560 Leqi Shen, Tianxiang Hao, Tao He, Sicheng Zhao, Yifeng Zhang, pengzhang liu, Yongjun Bao,  
 561 and Guiguang Ding. Tempme: Video temporal token merging for efficient text-video retrieval.  
 562 In *The Thirteenth International Conference on Learning Representations*, 2025a. URL [https://openreview.net/](https://openreview.net/forum?id=1Vp97zz5i8)  
 563 [forum?id=1Vp97zz5i8](https://openreview.net/forum?id=1Vp97zz5i8).

564 Xiaoqian Shen, Yunyang Xiong, Changsheng Zhao, Lemeng Wu, Jun Chen, Chenchen Zhu, Zechun  
 565 Liu, Fanyi Xiao, Balakrishnan Varadarajan, Florian Bordes, et al. LongVU: Spatiotemporal  
 566 adaptive compression for long video-language understanding. In *Forty-second International*  
 567 *Conference on Machine Learning*, 2025b. URL [https://openreview.net/](https://openreview.net/forum?id=XzZC4gs1mf)  
 568 [forum?id=XzZC4gs1mf](https://openreview.net/forum?id=XzZC4gs1mf).

569 Hui Sun, Shiyin Lu, Huanyu Wang, Qing-Guo Chen, Zhao Xu, Weihua Luo, Kaifu Zhang, and Ming  
 570 Li. Mdp3: A training-free approach for list-wise frame selection in video-llms. *arXiv preprint*  
 571 *arXiv:2501.02885*, 2025.

572 Yucheng Suo, Fan Ma, Linchao Zhu, Tianyi Wang, Fengyun Rao, and Yi Yang. From trial to  
 573 triumph: Advancing long video understanding via visual context sample scaling and self-reward  
 574 alignment. In *Proceedings of the IEEE/CVF International Conference on Computer Vision*, 2025.

575 Xi Tang, Jihao Qiu, Lingxi Xie, Yunjie Tian, Jianbin Jiao, and Qixiang Ye. Adaptive keyframe  
 576 sampling for long video understanding. In *2025 IEEE/CVF Conference on Computer Vision and*  
 577 *Pattern Recognition (CVPR)*, pp. 29118–29128, 2025.

578 Gemini Team, Petko Georgiev, Ving Ian Lei, Ryan Burnell, Libin Bai, Anmol Gulati, Garrett Tanzer,  
 579 Damien Vincent, Zhufeng Pan, Shibo Wang, et al. Gemini 1.5: Unlocking multimodal under-  
 580 standing across millions of tokens of context. *arXiv preprint arXiv:2403.05530*, 2024.

581 Qwen Team. Qwen2 technical report. *arXiv preprint arXiv:2407.10671*, 2, 2024.

582 Lan Wang, Yujia Chen, Du Tran, Vishnu Naresh Boddeti, and Wen-Sheng Chu. Seal: Semantic  
 583 attention learning for long video representation. In *Proceedings of the Computer Vision and*  
 584 *Pattern Recognition Conference*, pp. 26192–26201, 2025a.

585 Weihang Wang, Zehai He, Wenyi Hong, Yean Cheng, Xiaohan Zhang, Ji Qi, Xiaotao Gu, Shiyu  
 586 Huang, Bin Xu, Yuxiao Dong, et al. Lvbench: An extreme long video understanding benchmark.  
 587 In *Proceedings of the IEEE/CVF International Conference on Computer Vision*, 2025b.

588 Yuetian Weng, Mingfei Han, Haoyu He, Xiaojun Chang, and Bohan Zhuang. Longvilm: Efficient  
 589 long video understanding via large language models. In *European Conference on Computer*  
 590 *Vision*, pp. 453–470. Springer, 2024.

594 Haoning Wu, Dongxu Li, Bei Chen, and Junnan Li. Longvideobench: A benchmark for long-  
 595 context interleaved video-language understanding. In A. Globerson, L. Mackey, D. Belgrave,  
 596 A. Fan, U. Paquet, J. Tomczak, and C. Zhang (eds.), *Advances in Neural Information Processing  
 597 Systems*, volume 37, pp. 28828–28857. Curran Associates, Inc., 2024.

598 Mingze Xu, Mingfei Gao, Shiyu Li, Jiasen Lu, Zhe Gan, Zhengfeng Lai, Meng Cao, Kai Kang,  
 599 Yinfei Yang, and Afshin Dehghan. Slowfast-llava-1.5: A family of token-efficient video large  
 600 language models for long-form video understanding. *arXiv preprint arXiv:2503.18943*, 2025.

601

602 Jiaibo Ye, Haiyang Xu, Haowei Liu, Anwen Hu, Ming Yan, Qi Qian, Ji Zhang, Fei Huang, and  
 603 Jingren Zhou. mPLUG-owl3: Towards long image-sequence understanding in multi-modal large  
 604 language models. In *The Thirteenth International Conference on Learning Representations*, 2025.  
 605 URL <https://openreview.net/forum?id=pr37sbuhVa>.

606 Sicheng Yu, CHENGKAI JIN, Huanyu Wang, Zhenghao Chen, Sheng Jin, ZHONGRONG ZUO,  
 607 XU XIAOLEI, Zhenbang Sun, Bingni Zhang, Jiawei Wu, et al. Frame-voyager: Learning to  
 608 query frames for video large language models. In *The Thirteenth International Conference on  
 609 Learning Representations*, 2025.

610

611 Boqiang Zhang, Kehan Li, Zesen Cheng, Zhiqiang Hu, Yuqian Yuan, Guanzheng Chen, Sicong  
 612 Leng, Yuming Jiang, Hang Zhang, Xin Li, et al. Videollama 3: Frontier multimodal foundation  
 613 models for image and video understanding. *arXiv preprint arXiv:2501.13106*, 2025a.

614 Kaichen Zhang, Bo Li, Peiyuan Zhang, Fanyi Pu, Joshua Adrian Cahyono, Kairui Hu, Shuai Liu,  
 615 Yuanhan Zhang, Jingkang Yang, Chunyuan Li, et al. Lmms-eval: Reality check on the evalua-  
 616 tion of large multimodal models. In *Findings of the Association for Computational Linguistics:  
 617 NAACL 2025*, pp. 881–916, 2025b.

618 Shaolei Zhang, Qingkai Fang, Zhe Yang, and Yang Feng. LLaVA-mini: Efficient image and  
 619 video large multimodal models with one vision token. In *The Thirteenth International Confer-  
 620 ence on Learning Representations*, 2025c. URL <https://openreview.net/forum?id=UQJ7CDW8nb>.

621

622 Yuanhan Zhang, Jinming Wu, Wei Li, Bo Li, Zejun Ma, Ziwei Liu, and Chunyuan Li. Llava-video:  
 623 Video instruction tuning with synthetic data. *Transactions on Machine Learning Research*, 2025d.

624

625 Yunzhu Zhang, Yu Lu, Tianyi Wang, Fengyun Rao, Yi Yang, and Linchao Zhu. Flexselect: Flexible  
 626 token selection for efficient long video understanding. *arXiv preprint arXiv:2506.00993*, 2025e.

627

628 Zhisong Zhang, Yan Wang, Xinting Huang, Tianqing Fang, Hongming Zhang, Chenlong Deng,  
 629 Shuaiyi Li, and Dong Yu. Attention entropy is a key factor: An analysis of parallel context  
 630 encoding with full-attention-based pre-trained language models. In *Proceedings of the 63rd An-  
 631 nual Meeting of the Association for Computational Linguistics (Volume 1: Long Papers)*, pp.  
 632 9840–9855, Vienna, Austria, July 2025f. Association for Computational Linguistics. ISBN 979-  
 633 8-89176-251-0. doi: 10.18653/v1/2025.acl-long.485. URL [https://aclanthology.org/2025.acl-long.485/](https://aclanthology.org/2025.acl-long.485).

634

635 Junjie Zhou, Yan Shu, Bo Zhao, Boya Wu, Zhengyang Liang, Shitao Xiao, Minghao Qin, Xi Yang,  
 636 Yongping Xiong, Bo Zhang, et al. Mlvu: Benchmarking multi-task long video understanding.  
 637 In *Proceedings of the Computer Vision and Pattern Recognition Conference*, pp. 13691–13701,  
 638 2025.

639

640 Heqing Zou, Tianze Luo, Guiyang Xie, Fengmao Lv, Guangcong Wang, Junyang Chen, Zhuochen  
 641 Wang, Hansheng Zhang, Huaijian Zhang, et al. From seconds to hours: Reviewing mul-  
 642 timodal large language models on comprehensive long video understanding. *arXiv preprint  
 643 arXiv:2409.18938*, 2024.

644

## A APPENDIX

645 In this appendix, we provide additional implementation details, additional results, and more ablation  
 646 studies. For the use of large language models, we use LLMs only for language polishing.

648 A.1 ADDITIONAL IMPLEMENTATION DETAILS  
649650 We firstly provide additional implementation details. We use the Qwen2-7B-Instruct model to score  
651 the relevance between each frame’s caption and the question text. Prompts for LLM:  
652

```

653 prompt_ind = (
654     f"You are an expert in image-text matching.\n"
655     f"Question: {question}\n"
656     f"Image Caption: {caption}\n"
657     f"Please evaluate the relevance between the image caption and the
658         question by giving a score from 0 to 10, "
659     f"where 10 means highly relevant and 0 means completely
660         irrelevant. Please respond with a single number only, without
661         explanation."
662 )
663
664 prompt_con = (
665     "You are an expert in understanding events in long videos.\n"
666     "Below is a sequence of frames (described with captions), listed
667         in the order they appear in the video.\n"
668     "You are given a question about the video. Please judge how
669         relevant the **middle frame** is to the question.\n"
670     "Give a score between 0 (not relevant at all) and 10 (highly
671         relevant).\n\n"
672     f"Question: {question}\n\n"
673     f"Frame sequence:\n"
674     f"{context_text}\n\n"
675     f"The middle frame is Frame {len(prev_caps)+1}.\n"
676     f"How relevant is this frame to the question?\n"
677     f"Answer with a single number (0-10) :"
678 )

```

678 We use the LMMs-Eval (Zhang et al., 2025b) evaluation suite to test several Video-LLMs on differ-  
679 ent benchmarks.

680 Table 4: Results of our SeViCES with the three Video-LLMs on four datasets.

681 682 Model	683 VideoMME			684 MLVU	685 LongVB	686 LVBench
	687 Medium	688 Long	689 Overall	690 M-Avg	691 Val	692 Overall
693 Qwen2.5-VL-7B	62.6	53.1	63.5	63.9	60.2	41.0
694 + SVCFS (TAS-FS)	64.3 $\uparrow$ 1.7	54.8 $\uparrow$ 1.7	64.4 $\uparrow$ 0.9	69.3 $\uparrow$ 5.4	62.0 $\uparrow$ 1.8	44.9 $\uparrow$ 3.9
695 + SVCFS (CgMI-FS)	63.9 $\uparrow$ 1.3	56.2 $\uparrow$ 3.1	64.4 $\uparrow$ 0.9	71.4 $\uparrow$ 7.5	62.6 $\uparrow$ 2.4	44.7 $\uparrow$ 3.7
696 + SeViCES (SVCFS+ACR)	65.3 $\uparrow$ 2.7	56.8 $\uparrow$ 3.7	65.5 $\uparrow$ 2.0	72.2 $\uparrow$ 8.3	63.9 $\uparrow$ 3.7	45.4 $\uparrow$ 4.4
-----						
697 LLaVA-Video-7B	62.3	53.0	64.4	67.9	58.9	43.1
698 + SVCFS (TAS-FS)	62.9 $\uparrow$ 0.6	55.0 $\uparrow$ 2.0	64.8 $\uparrow$ 0.4	71.0 $\uparrow$ 3.1	61.8 $\uparrow$ 2.9	46.4 $\uparrow$ 3.3
699 + SVCFS (CgMI-FS)	63.2 $\uparrow$ 0.9	55.8 $\uparrow$ 2.8	64.5 $\uparrow$ 0.1	71.6 $\uparrow$ 3.7	61.5 $\uparrow$ 2.6	46.3 $\uparrow$ 3.2
700 + SeViCES (SVCFS+ACR)	64.7 $\uparrow$ 2.4	56.1 $\uparrow$ 3.1	65.6 $\uparrow$ 1.2	73.1 $\uparrow$ 5.2	63.1 $\uparrow$ 4.2	47.3 $\uparrow$ 4.2
-----						
701 InternVL2.5-8B	—	52.8	64.2	68.7	59.3	43.4
702 + SVCFS (TAS-FS)	62.4	55.2 $\uparrow$ 2.4	64.4 $\uparrow$ 0.2	72.0 $\uparrow$ 3.3	60.9 $\uparrow$ 1.6	46.5 $\uparrow$ 3.1
703 + SVCFS (CgMI-FS)	62.7	54.2 $\uparrow$ 1.4	64.2	71.5 $\uparrow$ 2.8	59.8 $\uparrow$ 0.5	45.0 $\uparrow$ 1.6
704 + SeViCES (SVCFS+ACR)	63.2	55.2 $\uparrow$ 2.4	64.7 $\uparrow$ 0.5	72.1 $\uparrow$ 3.4	61.7 $\uparrow$ 2.4	46.7 $\uparrow$ 3.3

697 A.2 ADDITIONAL RESULTS  
698699 Then, we provide additional results of SeViCES evaluated with three different Video-LLMs across  
700 four long video understanding datasets, as shown in Table 4. We report detailed performance for  
701 each component of our framework, including the Temporal-Aware Semantic Frame Selection (TAS-  
FS), Cluster-Guided Mutual Information Frame Selection (CgMI-FS), and the Answer Consensus

702 Refinement (ACR) module. These results further validate the contribution of each component and  
 703 highlight the robustness of SeViCES across diverse settings.  
 704

705 **A.3 MORE ABLATION STUDIES**  
 706

707 We further conduct ablation studies on the design choices of the semantic-based frame selection  
 708 strategy (TAS-FS). As shown in Table 5, we first compare two LLM scoring strategies: frame-  
 709 independent scoring and temporal-context scoring. The results show that temporal-context scoring  
 710 slightly outperforms frame-independent scoring, particularly on medium-length videos, while the  
 711 two perform comparably on very long videos. We speculate that this is because the time window  
 712 used ( $w = 5$ , i.e., 5 seconds) remains relatively short compared to the duration of very long videos  
 713 ( $\sim 40$  minutes).

714 Second, we examine the effect of combining the two scoring strategies. The results in the last two  
 715 rows indicate that the combination of frame-independent and temporal-context scoring substantially  
 716 improves performance over either strategy alone. Finally, incorporating the section-wise selection  
 717 scheme yields the best overall performance, confirming the effectiveness of ensuring both local  
 718 coverage and global relevance in semantic frame selection.

719 Table 5: Performance changes with different TAS-FS design strategies on VideoMME dataset.

Method	Overall	Medium	Long
Qwen2.5-VL	63.5	62.6	53.1
+ TAS-FS (frame-independent scoring)	63.5	61.7	54.4
+ TAS-FS (temporal-context scoring)	63.8	63.3	54.3
+ TAS-FS (rank scores and select top-64)	64.3	63.7	55.2
+ TAS-FS (section-wise selection, used)	64.4	64.3	54.8